(Remote Sensing of Clouds and Atmosphere, Sept 20-23, 1999, Firenze, Italy)

Far infrared measurements of cirrus

I. G. Nolt[a*] , M. D. Vanek[a], N. D. Tappan[a], P. Minnis[a] , J. L. Alltop[a], P. A. R. Ade[b], C. Lee[b,+] , P. A. Hamilton[b] , K. F. Evans[c], A. H. Evans[c] , E. E. Clothiaux[d] A. J. Baran[e],

[a]NASA Langley, Hampton, Va 23681-0001
[b]Queen Mary and Westfield Colllege, Mile End Road, London E1 4NS, UK
[c]University of Colorado, Boulder, Co 80309-0311
Pennsylvania State University, University Park, Pa., 16802
[d]UK Meteorological Office, Bracknell, RG12 2SZ, UK

ABSTRACT

Improved techniques for remote sensing of cirrus are needed to obtain global data for assessing the effect of cirrus in climate change models. Model calculations show that the far infrared/sub-millimeter spectral region is well suited for retrieving cirrus Ice Water Path and particle size parameters. Especially useful cirrus information is obtained at frequencies below 60 cm^{-1} where single particle scattering dominates over thermal emission for ice particles larger than about 50 μm. Earth radiance spectra have been obtained for a range of cloud conditions using an aircraft-based Fourier transform spectrometer. The Far InfraRed Sensor for Cirrus (FIRSC) is a Martin-Puplett interferometer which incorporates a polarizer for the beamsplitter and can be operated in either intensity or linear polarization measurement mode. Two detector channels span 10 to 140 cm^{-1} with a spectral resolution of 0.1 cm^{-1}; achieving a Noise Equivalent Temperature of approximately 1K at 30 cm^{-1} in a 4 sec scan. Examples are shown of measured and modeled Earth radiance for a range of cloud conditions from 1998 and 1999 flights.

Keywords: Cirrus, Clouds, Far IR, Remote sensing, FTS spectroscopy,

1. INTRODUCTION

Estimates indicate high altitude ice clouds account for the majority of radiative cloud warming effects. The theoretical basis for the retrieval of cirrus properties from microwave/sub-millimeter (sub-mm) radiance spectra using realistic particle shapes is a recent development.[1] Model calculations show that the Far-Infrared(Far-IR)/sub-mm spectral region (100 μm < wavelength < 1000 μm) is optimally suited for cirrus cloud observations since the measured radiance spectral response is close to the third moment, i.e. volume, of the particle size distribution. This contrasts with shorter wavelengths which operate in the geometric limit where the signal is proportional to particle area. As a result, less error exists in Ice Water Path (IWP) due to particle size, shape and phase function uncertainties compared with visible and IR methods. Since surface radiation variations are effectively blocked by water vapor absorption, the radiation background spectrum below the cirrus is relatively uniform for distinguishing the spatially variable cirrus signal in the sub-mm windows. At sub-mm wavelengths the ice particle emission and cloud temperature are relatively unimportant as a result of the reduced absorptivity of ice at these wavelengths. Finally, this spectral range provides the best particle size resolution for particle sizes greater than 50 μm, a size range not well resolved by either visible/IR or radar data. The purpose of this paper is to show a representative sample of Earth radiance measurements in this spectral range, and some preliminary comparisons to model calculations.

---

* For further information -
I. G. N. (correspondence): i.g.nolt@larc.nasa.gov: Tel: 757-864-1623; Fax: -8818
P. A. R. A.: para@qmw.ac.uk
K. F. E.: evans@nit.colorado.edu; http://nit.colorado.edu
+ C. L. is supported by a Royal Society Dorothy Hodgkin Fellowship.

2. FAR INFRARED CIRRUS PROPERTIES

As viewed from a high altitude aircraft or space platform, the Earth upwelling spectral radiance in the Far-IR mirrors the atmospheric temperature at the altitude where the optical depth saturates. The main radiance components are:

1. Radiation from tropospheric water vapor which mirrors the brightness temperature at optical depths defined by water vapor rotational transitions and the water vapor continuum opacity;
2. A possible black-body-like component from highly emissive liquid water cloud tops if not shielded by the vapor opacity;
3. A broad-featureless reduction in the radiance from scattering by ice (cirrus) particles;
4. Impressed upon these components are a number of relatively narrow water vapor and ozone rotational transition features arising from their concentrations in the upper troposphere and stratosphere.

Figure 1 is a model calculation of brightness temperature viewed from 12.5 km for a mid-latitude winter atmosphere containing a cirrus cloud between 9 and 10 km altitude[2]. The cirrus layer, characterized by a median mass equivalent diameter (Dme) of 100 μm and IWP of 10 g/m^2, implies a visible optical depth of ≈ 0.5. In this case the maximum temperature depression occurs in the "window" region of 45 cm^{-1}.

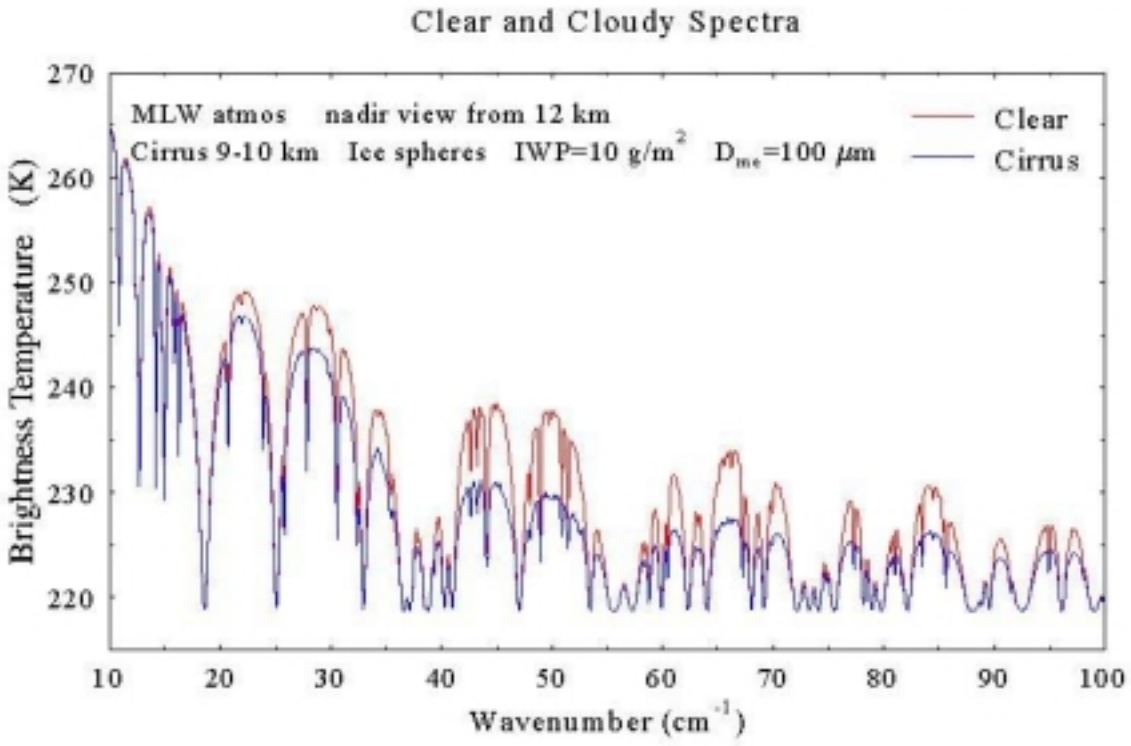

Figure 1: Model calculation of clear and cirrus radiance in terms of the brightness temperature as viewed in the nadir direction from 12.5 km altitude. The reduction in brightness temperature is the result of Mie type scattering of the upwelling radiation . The regions of strong absorption saturate at the tropopause temperature of 220K and are not sensitive to the presence of cirrus at lower altitude.

3. THE FAR INFRARED SENSOR FOR CIRRUS (FIRSC) INSTRUMENT

The objective of this international collaborative effort is to obtain sub-mm radiances from cirrus, develop cirrus property retrieval methods, and validate these remotely sensed properties with other measurements. A major task for the measurement program was to design a Fourier Transform Spectrometer (FTS) aircraft instrument to measure the upwelling far-infrared spectral radiance spectrum from an aircraft platform. A spectral resolution of 0.1 cm-1 is required to resolve the typical pressure-broadened lines of gaseous absorption features, primarily due to water vapor. The most difficult requirement was for a spectral Noise Equivalent Temperature sensitivity (NEΔT) of order 1K within a scan time of a few seconds. The short scan time is necessary to resolve cloud changes equivalent to less than 1 km at the typical airspeeds for a jet aircraft.

A FTS instrument can provide the wide spectral range and optimal resolution for radiance spectra measurements which span the Far-IR/submm atmospheric windows at wavelength longer than 100 μm (i.e. frequencies less than 100 cm^{-1} or 3000 GHz). Furthermore, a polarizing FTS instrument if used in a slant path viewing mode can provide particle shape information from vertical and horizontal linear polarization measurements. In a Martin-Puplett configuration dihedral (roof-top) mirrors replace the usual flat mirrors of a Michelson configuration and the instrument can be operated either in intensity or polarization sensitive modes.[3] The FIRSC FTS was built in a collaborative NASA and university effort. The cryogenic detector system was designed by Queen Mary and Westfield College based upon a similar system developed for the European SAFIRE-Airborne program.[4]

The FIRSC instrument uses two spectral channels to span the range between 10 and 140 cm^{-1}, the lower range from 10 to 70 cm^{-1} being sensed with a bolometer cooled to 0.3 K, and the 80 to 135 cm^{-1} range with an unstressed Ge:Ga photodetector cooled to 4.2 K. Cold optics and filtering inside the dewar define the field-of-view and spectral bandpass. Calibration is provided by scans with the reference port blackbody adjusted in flight to two known temperatures and an ambient temperature blackbody shutter inserted into the sky port. The polyethylene window is not included in the in-flight calibration path. Thus the transformation of measured sky spectra to calibrated sky brightness temperature is complicated by the need to correct for the emissivity and transmission of the polyethylene window. The other major calibration parameter is emissivity of the reference blackbody.

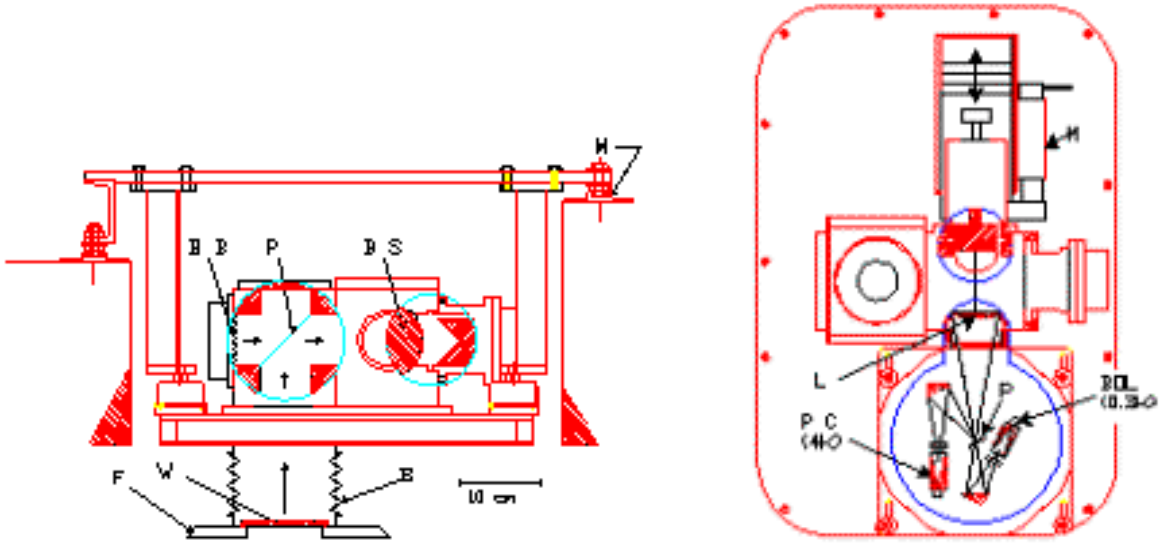

Figure 2: FIRSC optical configuration. The instrument is attached with vibration isolating mounts (M) to the plane floor and views the upwelling cloud radiance through a polyethylene window (W) installed in the fuselage (F). The input polarizer (P) combines one polarization component of the sky with an orthogonal component from the reference blackbody (BB) as input to the beamsplitter (BS) which is a free standing wire grid polarizer. An f/4 polyethylene lens (L) has a focus at polarizer (P) from which the signals are re-imaged to the two detectors.

The blackbodies are a QMW-developed material consisting of carbon-filled epoxy material with an inverted pyramidal surface. The measured emissivity is 98% at 10 cm^{-1} rising to 99.5% at 40 cm^{-1}. Further measurements of the reference blackbody emissivity are planned as an uncertainty of only 1% translates to a 2.5 K uncertainty in the calibration to absolute brightness temperature. Table 1 summarizes the observing parameters for FIRSC.

TABLE 1: Measurement and Instrument Parameters

Parameter	FIRSC
Bands (cm^{-1})	Band 1: 10-70(1998) Band 1: 10-35 (1999) Band 2: 80 – 135
Resolution (cm-1)	0.10
Field of View (radian)	0.03
Footprint (km)	< 1
Input Aperture (cm diam)	5.4
Scan Time (sec)	4
Max Opt. Path Diff (cm)	± 5
Max Mirror Stroke (cm)	± 2.5
Mirror Scan Vel (cm/sec)	1.25 (10 max)
Detectors	Band 1: Bolometer @ 0.3K Band 2: Ge:Ga PC @ 4K
Single Scan NEΔT	≈ 1K rms at 30 cm^{-1}

4. CLOUD RADIANCE MEASUREMENTS

Engineering and initial science flights of the FIRSC instrument were conducted in Apr-May, 1998, using NASA's T-39 (Sabreliner) aircraft at the Wallops Flight Facility. Following this series, a number of improvements were made for the Spring, 1999, flights. Since the Sabreliner was no longer available, the instrument was reconfigured for installation in a Lear Model 25C leased from Flight International, Inc. A general objective in the flights was to obtain correlative data by overflights of the Penn State 94 GHz radar and/or LaRC lidar accompanied by coincident radiosondes. Flights were also co-ordinated to coincide if cirrus conditions were forecast with overpasses of the UK ERS-2 Along Track Scanning Radiometer (ATSR) satellite.

In the 1999 series of seven flights, five flights were made with cirrus forecast at Penn State, one flight over LaRC for clear sky calibration, and one flight to measure linear polarization of cirrus. The duty cycle in 1999 was increased to have full resolution (0.1 cm^{-1}) interferograms sampled at 0.8 km intervals (5 sec intervals) along track compared to a 2.5 km sampling interval in 1998. Another important modification for 1999 was to increase the low frequency channel sensitivity by reducing the band's high frequency cut-off from 70 to 35 cm^{-1}. With these changes and improved shielding against electromagnetic interference, the in-flight noise levels in 1999 essentially matched laboratory performance. The level of single scan noise is shown in Figure 3.

From the flights to-date, three examples have been selected to illustrate the range of radiance spectra in the case of no cirrus, thin cirrus, and ice clouds associated with a deep convective and precipitating front.

4.1 Clear sky and thin cirrus:
Examples of measured and calibrated radiance spectra are shown in Figure 3 for a clear sky over NASA Langley, May 27, 1999 (F17), and a visibly transparent but deep cirrus cloud over Penn State University , Apr 15, 1999 (F13). Coincident radiosondes were obtained for both cases. Figure 3 compares averages of 10 (50 sec or 8 km track) measured uncalibrated spectra from 12.5 km altitude. The lower trace records the in-flight measured single 4 sec scan noise level which equates to a spectral Noise Equivalent Temperature (NEΔT) precision of 1K at 30 cm^{-1} and 7K at 10 cm^{-1} for a spectral resolution (unapodized) of 0.1 cm^{-1}.

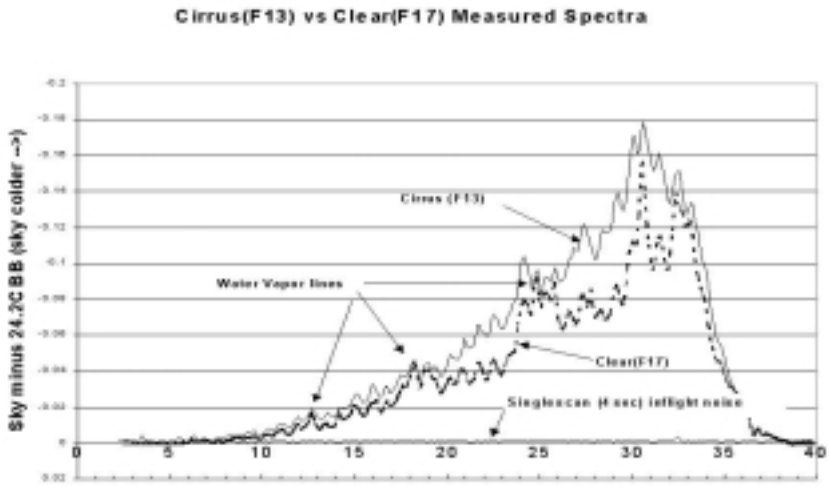

Figure 3: Measured spectra averaged over 8 km from 41,000 ft altitude for clear and cirrus conditions. The measured signal is the intensity difference of the sky source minus the reference blackbody. The regions of strong water line emission are insensitive to conditions beyond a short distance. The results show the frequency squared dependence expected for the Planck function at these frequencies and periodic channel fringe from the PE window with ≈ 0.8 cm^{-1} period.

Figure 4 below shows the GOES satellite visible image and radiosonde sounding at the time of Flight 13.

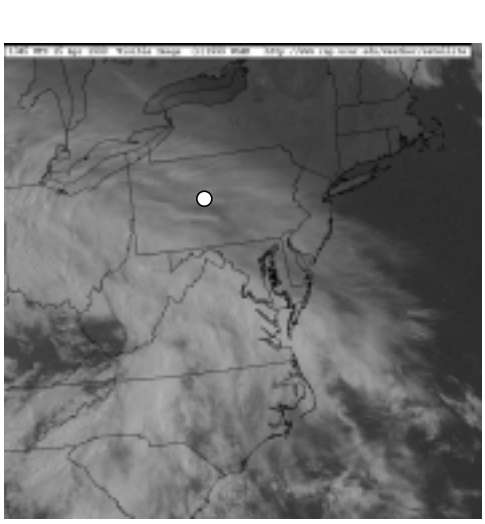

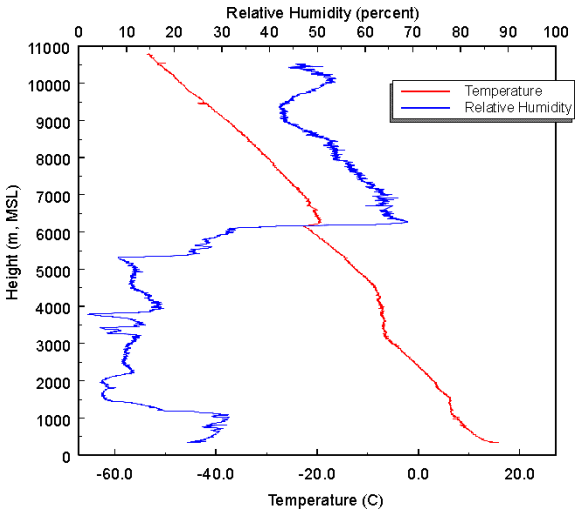

Figure 4: GOES Visible image and radiosonde data for the flight on Apr 15, 1999 (F13). The dot indicates the location of the measurement and the radiosonde data provided by Penn State.

The conversion of measured radiance difference to absolute temperature requires accurate measurements of the emissivity of the reference blackbody and the transmission/emissivity of the polyethylene fuselage window. Figure 5 shows the current calibration of the clear sky measurement to the radiance calculated using the radiosonde temperature/humidity profiles and Hitran line database. The very centers of the strongest water line centers at 18.6 and 25 cm^{-1} are difficult to model due to absorption within the instrument.

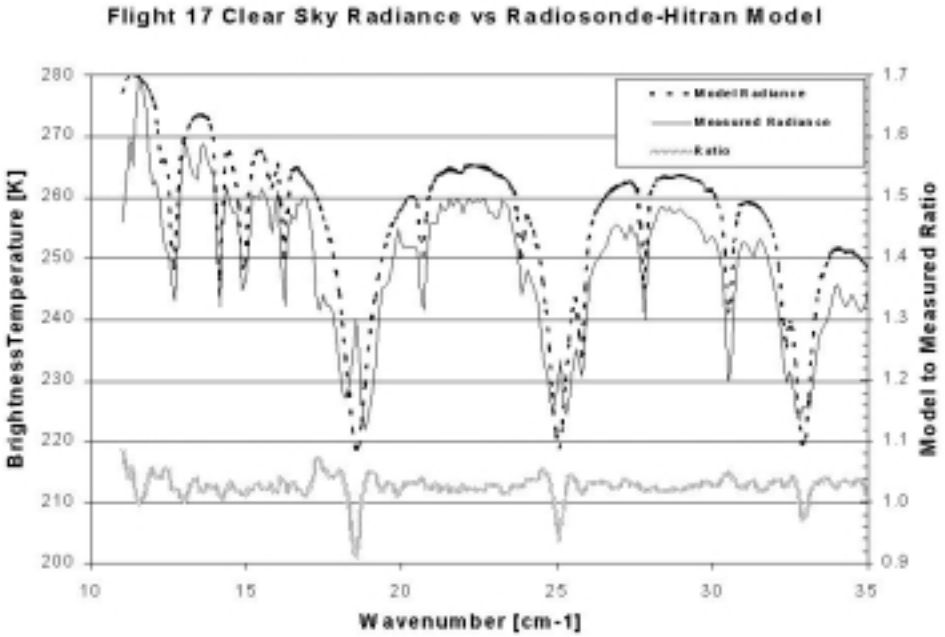

Figure 5: The clear sky radiance (F17) shown in Figure 3 converted to absolute brightness temperature and compared to the radiance calculated from coincident radiosonde data and the Hitran spectral line database.

The calibration in Figure 5, which uses the current best measurements of the blackbody emissivity and window transmission, agrees well with the principal spectral features but shows a temperature offset of about 6 C. This difference could be the result of as little as a 2 % bias in the combined blackbody emissivity, window transmission, and radiosonde data. A future redesign of FIRSC will hopefully eliminate the window external to the in-flight calibration path. However, a very accurate measurement of the reference blackbody emissivity is a fundamental requirement.

Figure 6 compares calibrated radiances for the measured spectra in Figure 3. No retrievals for cirrus parameters have been made for the Flight #13 data in Figure 6. Thus we do not know the relative effect of cirrus and water vapor profile differences in producing the approximate 20K lower brightness in the sub-mm windows (e.g.22 and 30 cm-1) seen here. The brightness temperature difference appears to be a maximum near 30 cm-1, suggestive of a median particle size near 200 μm. It is possible that the coincident Penn State 94 GHz cloud radar data when fully analyzed will provide some validation.

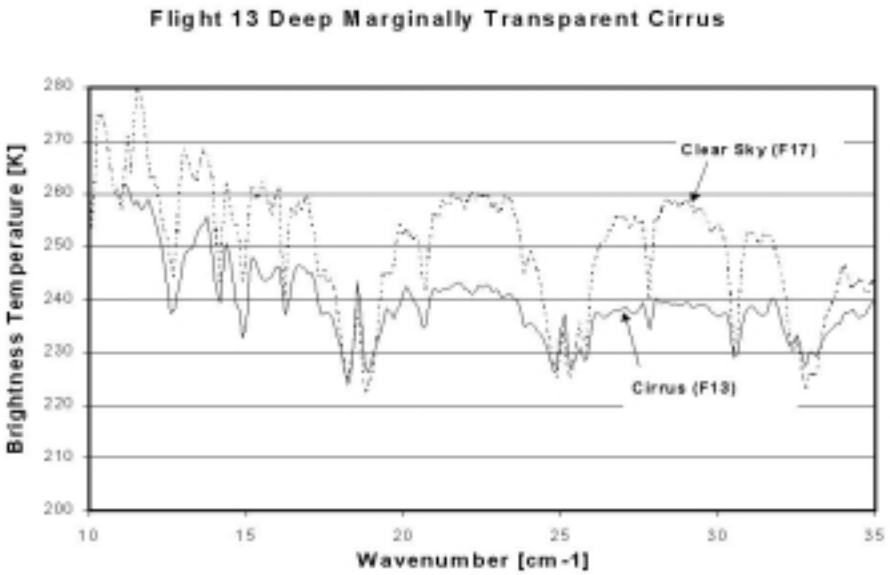

Figure 6: Comparison of similarly calibrated cirrus and clear sky radiance for the measured spectra in Figure 3. The temperature differences of about 20 C in the cirrus-sensitive windows are substantiated by equal brightness temperatures in regions of strong water line emission (e.g. 18.6, and 25 cm^{-1}) which are not sensitive to cirrus.

4.2 Deep Ice Clouds of a Precipitating Frontal System:

A flight from the 1998 series provides our best example to-date of very cold brightness temperatures encountered over deep ice clouds. In this case our flight segment included both clear sky and the deep ice clouds associated with a precipitating frontal system for which the satellite IR image is shown in Figure 7.

GOES-8 IR Image over Eastern US, 1545 UTC, May 27, 1998

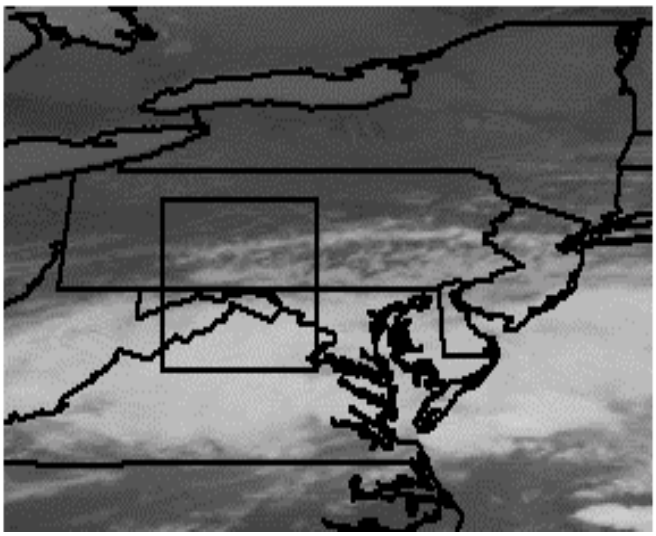

Figure 7: IR Image of Frontal System. The front was moving south but with a 70 kt wind from west at the cirrus top of 12.5 km. The flight segment started in the NE corner and terminated at the SW of the highlighted box.

Figure 8 compares a scan (#205) over clear sky at the NE corner of the highlighted box on the satellite image and two scans (#295 and 297) obtained 20 min later over the front. Each spectrum was obtained in a sampling length along the flight track of

approximately 0.7 km (4 sec) and repeated every 2.5 km (cycle time of 14 sec). Thus the two latter scans are separeated by 5 km along the flight track. This flight also coincided with an ATSR overpass.

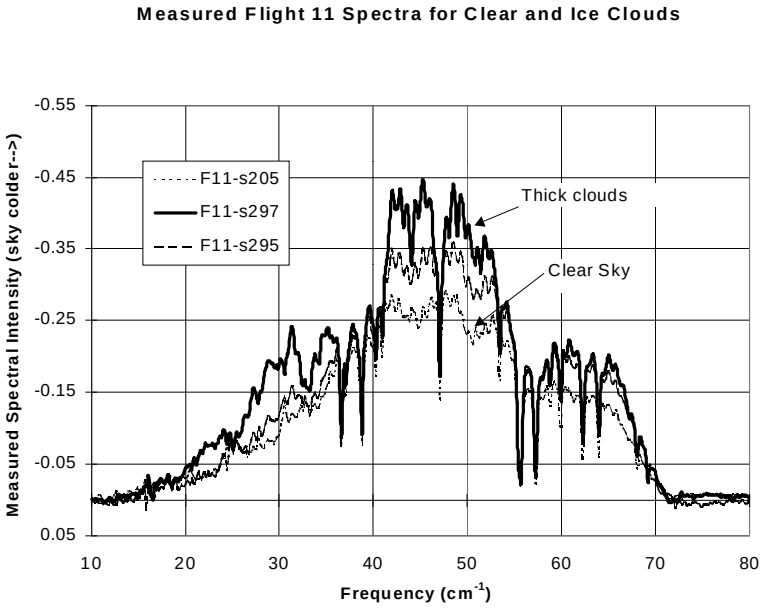

Figure 8: Measured spectral intensities where the upwelling radiance is relative to a reference blackbody at 17C. The result shows very large window temperatures changes with little change in the strong water lines.

An early version of calibration for this data is shown in Figure 9. The result shows residual fringing from the window and also deviates at higher frequencies from the tropospheric temperature, known from a radiosonde to be about 215 K. Nevertheless, the data show that very large brightness temperatures can occur over deep ice clouds.

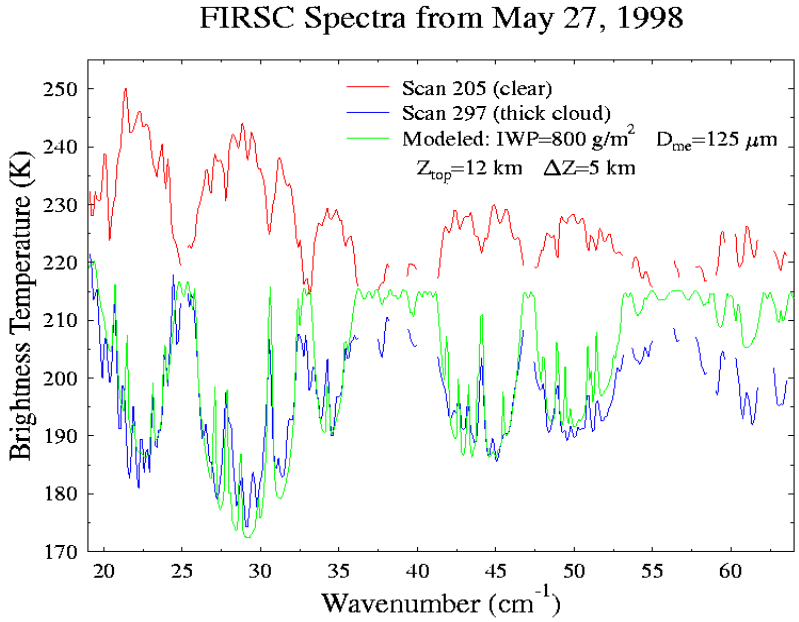

Figure 9: Brightness temperature for thick cloud scans shown in Figure 8. This early calibration result is not properly corrected for the window transmission and emissivity which likely accounts for the deviation from the model spectrum at frequencies above 35 cm-1. The ice cloud parameters and model fit are also shown for a preliminary retrieval.

An important parameter in designing remote sensing technology for cirrus is the scale of its variability. In addition to very large temperature depressions this flight over a strong convective front showed unusually large radiance changes on a sampling scale of 2.5 km. Figure 10 shows the change in the average brightness temperature in 3 sub-mm windows for this flight segment. Many factors could influence the brightness temperature but the changing relative values of the different frequency bands is suggestive of variability in particle size. It should be noted that other flights, all over non-convective systems, have shown little variability over distance scales of 10 km.

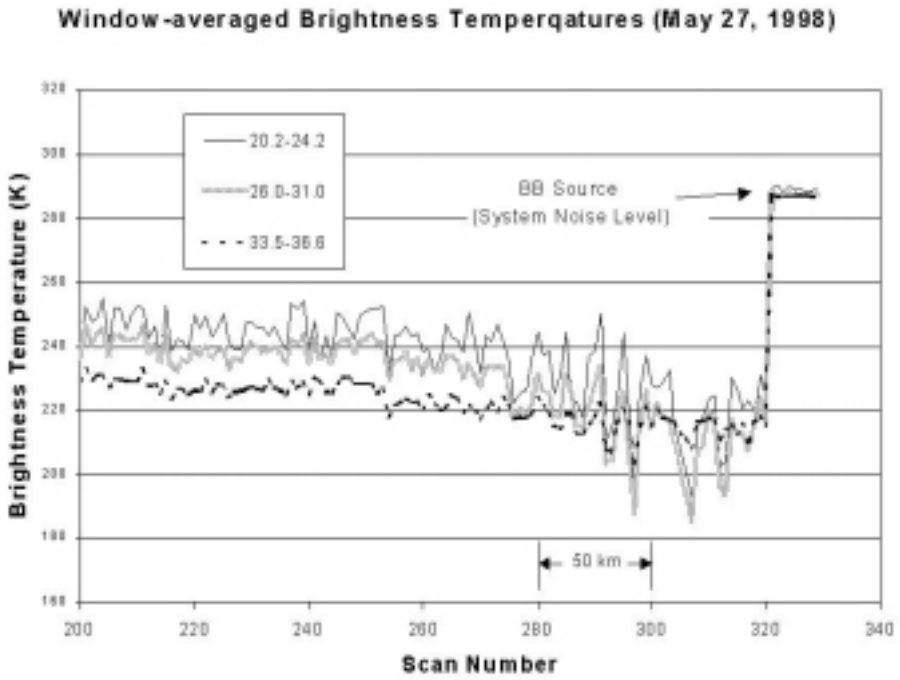

Figure 10: Brightness temperatures in three far-infrared windows along the indicated flight track segment. Scans were obtained at approximately 2.5 km intervals along the flight track.

4.3 Cirrus Polarization Measurements

Theoretical models for cirrus scattering predict that non-spherical ice particle will be aligned aerodynamically with the longer particle axes horizontal[5]. Consequently if viewed along a slant path columnar particles will show enhanced scattering, i.e. colder brightness, for horizontally polarized (H) than for vertically polarized (V) radiation. The following figure is a measurement of polarization intensity difference along a slant path 70 degrees from nadir. This data was obtained June 3, 1999, on a flight track along the N-S axis of an eastwardly advancing front over central Virginia.

The H-V linear polarization difference was recorded on the northbound leg (with a mirror replacing the input polarizer in the configuration in Figure 2) followed by a measurement of the H intensity on the reverse track. The track covered clear areas at the northern terminus and these two measurements define the H and V temperature depressions associated with the segment over cirrus.

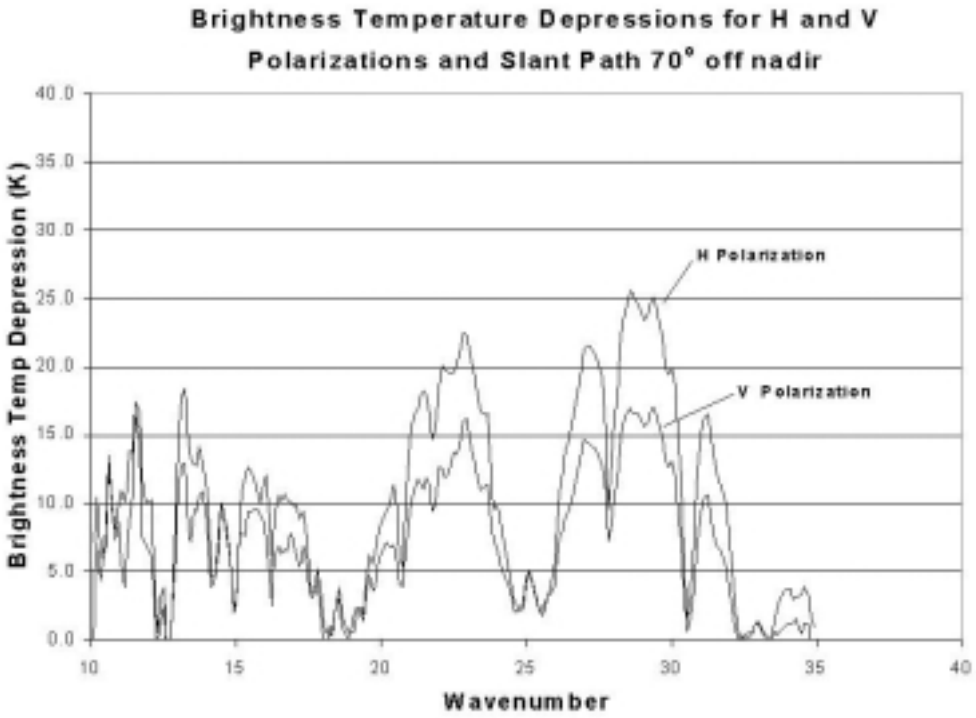

Figure 11: Temperature Depression for H and V linear polarization observed at 70^{o} from nadir. The H depression is the difference between spectra for clear sky and visually thin cirrus. The V temperature depression is based on the measured differential H minus V polarization for cirrus on the reverse flight leg. Averages of 12 spectra (1 min or 10 km along track) for cirrus and clear segments were subtracted to generate the H polarization temperature depression, from which the subtraction of the H-V cirrus measured spectrum defines the V temperature depression.

5. CONCLUSIONS

The results to-date show the generally expected reductions in Earth radiance correlated with visual observations of the cirrus optical depth. In addition, the polarization of cirrus scattering at sub-mm wavelengths has been observed. Our current effort is focusing on understanding the calibration of the measured spectra to absolute brightness temperature where the reference blackbody emissivity and PE window properties are the major uncertainties. At the same time the program is exploring the instrument changes necessary to install FIRSC on a higher altitude aircraft such as the Proteus or ER-2. The current restriction to commercial aircraft altitudes of less than 43,000 ft enables cirrus overflights only during the winter/spring at mid-latitude, and excludes flights over tropical cirrus which occurs at higher altitudes. Retrieval analyses are planned for the next phase to investigate in more detail the correspondence to model radiances and the role of in-cloud water vapor in limiting the sensitivity at sub-mm wavelengths to lower cloud cirrus. This effort will also integrate into the analsyses available radiosonde and cloud radar data by the Penn State group, radiosonde data obtained by the LaRC lidar group, satellite imagery, and ATSR infrared sounding data.

In a parallel technology program this data is being used to evaluate and model a radiometer concept for cirrus measurements from space. In a joint effort with Goddard Space Flight Center, high temperature superconducting bolometer technology is being evaluated for this application[6]. These detectors, which require cooling to only 80K, appear to be sufficiently sensitive to measure the broadband “window” brightnesses (e.g. Figures 9 and 10) with a relatively modest size radiometer.

6. ACKNOWLEDGEMENTS

This work owes much to the co-operation and enthusiasm of many participants. The flight support by the NASA Wallops Flight Facility and Flight International, Inc. has been superb and willing to accommodate multiple stand-by days awaiting suitable cirrus. We especially appreciate the co-ordination with flight planning and auxiliary data acquisition provided by Bruce Worrell, Jr, of Flight International, Inc.; Doug Young of NASA Wallops Flight Facility; David Babb of the Penn State group; and John Wright of the UK ERS-2 satellite team. The excellent instrument performance reflects the expertise of Fred Gannaway, QMW, in detector system fabrication; Jesse Davis of Cochise Instr., Inc. in signal electronics design and fabrication; and Steve Predko of the Univ. of Oregon in interferometer component fabrication and aircraft installation. Financial support for this program has been provided by LaRC Director's Discretionary grants in 1998-99, and by the NASA Earth Science Enterprise and Earth Science Technology Office.

7. REFERENCES

1. Evans, K.F., and G.L. Stephens, "Microwave Radiative Transfer through Clouds Composed of Realistically Shaped Ice Crystals: Part II: Remote Sensing of Ice Clouds", J. Atmos. Sci., **52,** 2058-2072, 1995.
2. Evans, K. F., and A. H. Evans, B. T. Marshall, and I. G. Nolt, "The Prospect for Remote Sensing of Cirrus Clouds with a Submillimeter-wave Spectrometer," J. Appl. Meteor. **38**, pp. 514-525, 1999.
3. Martin, D.H., and E. Puplett, " Polarization Interferometric Spectrometer for Millimeter and Submillimeter Spectroscopy", Inf. Phys., **10**, pp 105-109, 1969.
4. Dickinson, P, B. Carli, P. Ade, I. Nolt, J. Leotin, and M. Carlotti, "SAFIRE-A An Airborne Far Infra-red Limb Sounder", S.P.I.E Volume 2586, pp. 214-224, *Global Process Monitoring and Remote Sensing of the Ocean and Sea Ice*, 25-28 Sept 1995, Paris, Fr.
5. Evans, K.F, S.J. Walter, A.J. Heymsfield, and M.N. Deeter, "Modeling of Submillimeter Passive Remote Sensing of Cirrus Clouds", J. Appl. Meteor., **37**, pp 184-205, 1998.
6. Brasunas, J., and B. Lakew, "High Tc Superconducting Bolometer with Record Performance," Appl. Phys. Lett., **64**, pp. 777-778, 1994.